2022 47th International Conference on Infrared, Millimeter and Terahertz Waves (IRMMW-THz) | 978-1-7281-9427-1/22/$31.00 ©2022 IEEE | DOI: 10.1109/IRMMW-THz50927.2022.9895702

Photonic Assisted Beam Steering Enabled by Hybrid Integration of InP-based Antenna Array and Polymer-based Optical Phased Array

S. Nellen[1], T. Qian[1], G. Schwanke[1], S. Lauck[1], D. de Felipe[1], M. Kleinert[1], M. Deumer[1], M. Baier[1], R. Kohlhaas[1], L. Liebermeister[1], N. Keil, M. Schell[1,2], and B. Globisch[1,2]

[1]Fraunhofer Institute for Telecommunications, Heinrich Hertz Institute, Einsteinufer 37, 10587 Berlin, Germany

[2]Technische Universität Berlin, Institut für Festkörperphysik, Hardenbergstraße 36, EW 5-1, 10623 Berlin, Germany

***Abstract* — Beam steering is advantageous for continuous-wave terahertz applications in sensing, imaging, and wireless communication. While wide spread in lower frequency bands, in the terahertz region complex emitter and receiver structures are hardly feasible with discrete devices, due to the shorter wavelengths. Therefore, we propose and demonstrate the use of photonic integration: A 1x4 antenna array based on photodiodes is driven by an optical phased array based on polymer. The packaged emitter features increased directivity and enables beam steering across 30 °.**

I. Introduction

Applications for continuous-wave (cw) terahertz technology evolved from purely spectroscopic analysis to a variety of scenarios e.g. in sensing, imaging and wireless communication. Especially solutions for real-world applications require higher complexity, improved stability and reduced size compared to tabletop systems in the laboratory. The photonic integration approach offers a comprehensive toolbox for miniaturization and integration since it exploits mature technologies used in optical fiber communication.

In this paper, we approach hybrid integration of a polymer-based waveguide network and an array of photodiodes (PDs) with integrated antennas based on indium phosphide (InP). Thus, enhanced antenna gain of the terahertz emitter (Tx) and purely photonic-controlled beam steering are realized. Whereas these features are also relevant for terahertz sensing and imaging, our work focuses on 300 GHz wireless communication. Here, a high antenna gain is desirable, because additional optical elements such as lenses or mirrors would increase the complexity and mechanical sensitivity of the link. Furthermore, beam steering capability allows for switching between receiver units in point-to-point scenarios or for scanning a certain area as requested in 5G and 6G scenarios.

II. Beam Steering and Chip Design

The basic concept of antenna arrays is the superposition of the radiated field of neighboring antennas [1]. The radiation pattern of the antenna array will be different from a single emitter due to angle dependent superposition of the fields. For an antenna pitch d below or in the range of the wavelength λ, the main lobe of the array will be narrower than the one of a single antenna, i.e. antenna gain is increased. Since the superposition of the fields is phase sensitive, changing the phases of the single antenna elements can be used to manipulate the resulting radiation pattern of the array, i.e. for beam steering. The relation between the resulting beam angle θ_0 and the properties of the array is $\cos(\theta_0) = -(\lambda / 2\pi)\cdot(\beta / d)$, where β is the respective phase difference between neighboring antennas.

In order to control the phase of a photonic terahertz antenna, the phase of the optical input signal needs to be controlled. Therefore, we designed and fabricated a polymer waveguide network (Fig. 1 (a)) in the PolyBoard platform, which includes multimode interferometers (MMIs) and thermo-optical phase shifters (PS) [2]. The polymer chip receives the signal from two single-mode lasers and provides a beat signal of those to each

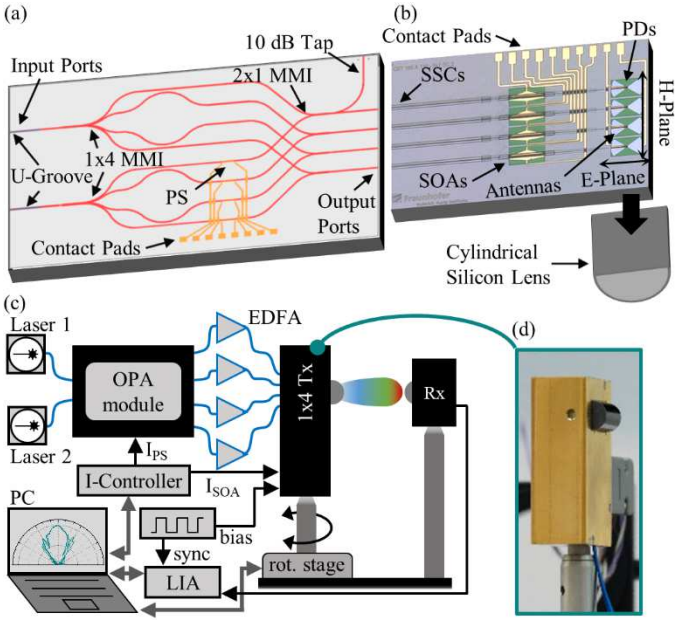

Fig. 1. (a) Layout polymer phase shifter: U-grooves at the input ports ease the fiber attachment at the polymer-based optical phased array (OPA). 1x4 MMIs split up each optical input. The lower optical path passes through four individually controllable phase shifters (PSs), 2x1 MMIs combine the respective signals from the upper and the lower inputs. The four output ports provide the same beat signal, but with different phase to the antenna chip. Gold-plated contact pads at the lower edge serve to electrically control the PSs. A 10 dB tap enables monitoring of the optical signal.
(b) Layout InP Antenna array: The micrograph shows the 2 mm x 3 mm InP antenna chip: the optical beat signal from the OPA channels is fed into the respective InP waveguide using the SSCs. SOAs are integrated between SSC and PD to boost the optical signal. The PDs are connected to bowtie antennas, which line up along their H-plane. The bias for the PDs and the driving current for the SOAs are applied via gold-plated pads at the upper edge. For proper coupling of radiation from InP substrate into air, the antenna chip is mounted on a cylindrical hyperhemispherical silicon lens (Ø 10 mm x 20 mm).
(c) Experimental setup: For characterization of the beam steering module, two single-mode lasers with 300 GHz frequency spacing are plugged to the OPA module. In order to compensate insertion and coupling losses, the OPA output signals are amplified by EDFAs (Thorlabs, EDFA100P) before feeding the Tx module. The Tx is mounted on a rotation stage (Thorlabs, PRMTZ8/M) 20 cm in front of the Rx, i.e. a Schottky barrier diode with silicon lens (ACST, A1). In order to use a lock-in amplifier (LIA, Signal Recovery 7265) for the Rx signal, the bias (-1 V) of the PDs is chopped with 20 kHz by a square wave generator (Keithley 3390). A PC controls the rotation stage, reads out the LIA, and sets the values for the SOA and PS currents via a current controller (Thorlabs, PRO8000). Radiation pattern for various settings of the PSs are acquired with 0.5 ° resolution.
(d) Packaged module: 1x4 Tx with optical fibers at the bottom and cylindrical silicon lens at the right side of the housing (58 mm x 33 mm x 20 mm).

978-1-7281-9427-1/22/$31.00 ©2022 IEEE

Authorized licensed use limited to: National Technical University of Athens (NTUA). Downloaded on December 07,2022 at 12:34:36 UTC from IEEE Xplore. Restrictions apply.

output port, whereas the PS can individually control the phase of each beat signal. Since this chip provides the optical signal for the phased array, it is called optical phased array (OPA).

The antenna array is realized on the generic InP foundry platform at Fraunhofer HHI, which provides the required photonic elements [3]: spot size converters (SSCs) for coupling light from fiber to chip, optical waveguides, semiconductor optical amplifiers (SOAs), and PDs. Fig. 1 (b) shows a micrograph of the fabricated antenna array. The pitch of the SSCs at the chip facet is 250 µm and enables either direct chip-to-chip coupling to the OPA, or coupling to a fiber array. The SOAs boost the optical signal before feeding it into the PDs. The SOAs are also used to individually adjust the radiation intensity of each PD. The PDs are integrated into the feeding point of the bowtie antenna [4]. In order to maintain 250 µm pitch between the antenna elements, bowties of reduced size are used. The impedance of the antennas is matched to the PDs around 300 GHz. Since the bowtie's dimension is smaller along its H-plane, the antenna array lines up along this axis. In order to couple the radiation from the InP substrate into air, the array chip is mounted on a cylindrical silicon lens, which is lens-shaped in the E-plane, but has a plane surface in the H-plane.

For the characterization of the antenna array, a metallic housing hosts chip and lens (Fig. 1 (d)), and a 1x4 fiber array is attached to the SSCs. Thus, the optical coupling is stable during the measurements, and allows for additional fiber amplifiers (EDFAs) between OPA and PDs. The additional boost is needed, as coupling and insertion losses were higher than expected and could not be compensated by the SOAs only. The OPA's output ports are also coupled to a fiber array. To connectorize the input ports, cleaved fibers are snapped into the U grooves in the polymer. Multi-pin sockets allow for electrical connection of the Tx and OPA during the measurement. The radiation pattern is measured for various settings of the antenna's phase difference β as described in Fig. 1 (c).

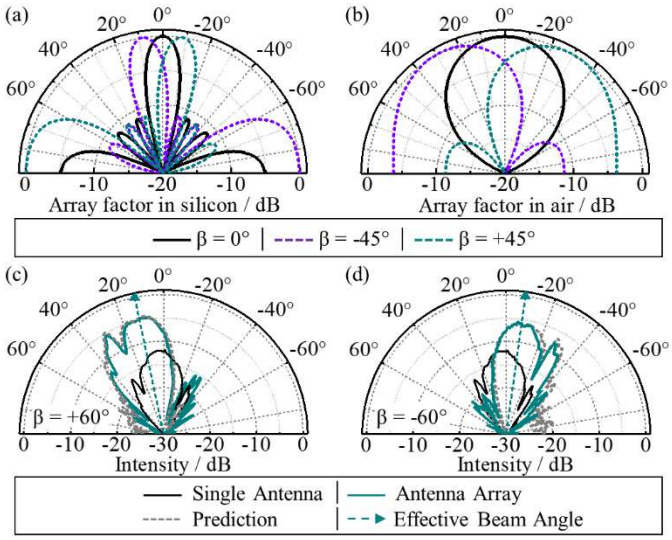

Fig. 2. (a) For radiation into a hemisphere of silicon, the array factor of the 1x4 array with the given antenna pitch of 250 µm and a target frequency of 300 GHz results in a narrow main lobe (15.5 °) and beam steering of ±8.4 ° for a phase difference of β = ±45 °. (b) For radiation into air, the main lobe is broadened (54 °) according to Snell's Law and the diffraction at the surface between silicon and air. After diffraction, the steering angle increases to ±30 ° for a phase difference of β = ±45 °. (c/d) The radiation pattern of a single antenna element (black) is measured as reference, before the H-plane of the 1x4 array (green) is characterized with a phase difference of β = +60 ° (c) and β = -60 ° (d). The dotted gray pattern is the theoretical prediction based on the calculated array factor. The green dotted arrow point toward the effective radiation angle, i.e. +18 ° and -12 ° with a respective penalty of -5 dB and -6 dB compared to straight radiation. The normalized intensity relates to the maximum power of the 1x4 emitter, i.e. +12 dB of a single emitter.

III. Results

Disregarding the particular radiation of the bowtie and assuming isotropic radiating antennas, the impact of the array properties on the radiation pattern can be calculated as the array factor (AF) [1]. Hence, a prediction of the radiation pattern of the particular antenna array results from the product of AF and the pattern of a single antenna. Fig. 2 (a) shows the AF, i.e. the radiation pattern of four isotropic radiators with 250 µm pitch at 300 GHz inside a half space of silicon. Side lobes arise at >60 ° off the center and the narrow main lobe can be tilted across 16.8 ° with a phase shift of β = ±45 °. However, Snell's Law applies for the transition from silicon lens into air. This results in a broadened main lobe (Fig. 2 (b)) due to diffraction towards higher angles. This effect also amplifies the beam steering and results in a total scan angle of 30 ° for β = ±45 °.

Fig. 2 (c) and (d) show the measured pattern of a single antenna (black) as reference. The dotted grey lines indicate the product of the AF and the pattern of a single antenna, i.e. the predicted array radiation. The measured radiation for a phase difference of β = ±60 ° (green lines) match very well with the predicted beam steering. Due to the non-isotropic character of the single radiators, the effective beam angle (green dotted arrows), i.e. the center of the 3dB-lobe, differs from the beam angle of the AF. Phase shifts of β = ±60 ° allow for a total scan angle of 30 °.

IV. Conclusion

We demonstrated photonic-enabled beam steering at 300 GHz with a polymer-based optical phased array and an InP-based 1x4 photodiode array with integrated antennas. The measured beam steering from -12 ° to +18 ° agrees with the theoretical prediction. Note, that the power of the tilted main lobe is still >6 dB higher than from a single emitter. The polymer and InP chips are suited for hybrid photonic integration. In the future, we plan to reduce the insertion loss, increase the gain of the integrated amplifier, and investigate alternatives to the silicon lens, in order to improve the radiation into air. The number of antenna elements will be increased to increase the directivity and the total power. In combination with less directive antenna elements, even higher beam angles are achievable. Thus, the photonic approach bears great potential for antenna arrays in scenarios for dynamic point-to-point communication.

References

[1] C. A. Balanis, "Arrays: Linear, Planar, and Circular," in *Antenna Theory: Analysis and Design*, 4th ed., no. February, John Wiley & Sons Inc, 2016, pp. 285–329.

[2] M. Kleinert *et al.*, "Photonic integrated devices and functions on hybrid polymer platform," in *SPIE OPTO*, 2017, vol. 10098, p. 100981A, doi: 10.1117/12.2256987.

[3] N. Grote, M. Baier, and F. Soares, "Photonic Integrated Circuits on InP," in *Springer Series in Optical Sciences*, vol. 161, Springer, Cham, 2017, pp. 799–840.

[4] S. Nellen *et al.*, "Radiation pattern of planar optoelectronic antennas for broadband continuous-wave terahertz emission," *Opt. Express*, vol. 29, no. 6, p. 8244, 2021, doi: 10.1364/oe.416844.

Authorized licensed use limited to: National Technical University of Athens (NTUA). Downloaded on December 07,2022 at 12:34:36 UTC from IEEE Xplore. Restrictions apply.